【Article】

Linear Perturbation on Axially Symmetric Vortices under A Uniform Gravity

TAKAHASHI Koichi

Abstract : The previous perturbative method to investigate the stability of vortex is extended so as to incorporate gravity in a uniformly rotating frame. The viscosity expansion method is employed, in which the radial and the z-components of the velocity field are proportional to viscosity and are therefore infinitesimally small, while the azimuthal component is independent of the viscosity. The rotation of the frame is incorporated by the Coriolis force. The algebraic eigenfrequency equation (EFE) of the sixth order is derived. There exist three physical eigenfrequencies that are generally coordinate dependent. The perturbations are found to be possible for the azimuthal wavenumber being equal to or greater than two. Since the real parts of the eigenfrequencies are dominantly positive and decreasing functions of the radial coordinate, the patterns of perturbations mainly form trailing spirals. Amplitudes of perturbations are also calculated. Their phases are shifted by the gravity.

1. Introduction

Vortices of macroscopic scales can be observed everywhere where viscous fluid exists. Whirlwind, tornado, typhoon (or cyclone) and eddying tide are the examples. Interacting with other vortices or with the environments, vortices evolve, stay steady and decay, thereby exhibiting generally quite complicated temporal behaviour.

From the meteorological point of view, typhoon, for example, is a very complex swirl of atmosphere that requires, together with input data, large amount of numerical calculations based on physical principles for describing and understanding its structure and behaviour. Although atmosphere is a fluid whose dynamics must be described in terms of a differential equation called the Navier-Stokes (N-S) equation, the evolution of typhoon is believed to be mainly derived by formation of cumuli resulting from the first order phase transition that is discontinuous in time and inaccessible to by the differential equations (Ooyama 1966). The interactions of typhoon with other numerous components of geophysical elements are also the cause of difficulty in analyzing and predicting the capricious phenomena. For a practical purpose of weather-forecasting, therefore, it is inevitable to rely not only on

statistical method but also to models parametrized for wind, pressure and so on (Holland 1980 ; Willoughby and Rahn 2004 ; Willoughby et al. 2005). Phenomenological modelings of this kind make it possible to construct numerically detailed view of evolving typhoons.

Nevertheless, we also know that the time-independent simple vortex model of typhoon is successful to capture such very fundamental characteristics of matured typhoon as the direction of swirling, the wind speed distribution, the eye formation, the correlation of the wind speed and the size of the eye and the existence of the warm core (Takahashi 2015a). Here, (frequently axisymmetric) solutions to the N-S equation that are transformed to a set of ordinary differential equations are referred to as simple vortices. The simple vortices are formed by laminar flow and are free from complexity due to turbulences. Irrespective of such over-simplification, they can be handy models of typhoons in large scales.

The dynamical evolution of a vortex is governed initially by its instability. Studies on this point exploiting numerical calculation method have required several simplifications because of the intrinsic complexity of atmospheric dynamics. Eady (1949) treated adiabatic perturbations on uniform flows in a rotating frame to study the vertical structure of the flow. Walko and Gall (1984) numerically studied the stability of two-dimensional vortices and found both of stable and unstable modes. Smith and Rosenbluth (1990) gave an exact solution of perturbation for $n = 1$ mode and showed that it is not exponentially but algebraically unstable. Nolan and Montgomery (2002) adopted a phenomenological background flow of incompressible fluid with low Reynolds numbers to model a typhoon. McWilliams et al. (2003) incorporated the Coriolis force for the inviscid vortices and calculated the eigenfrequency by taking account of the azimuthally averaged higher order perturbations. All works indicate that the steady and axisymmetric vortex is essentially unstable. However, analytic relations between eigenfrequencies of perturbations and the resultant unstable motions have yet been obtained for realistic three dimensional vortices.

Fortunately, some simple vortices have been known to exist as the exact solutions to the N-S equation. The simplest ones among the simple vortices are the steady and axially symmetric vortices with no boundaries constructed by Burgers (1948), Sullivan (1959) and Takahashi (2014). Takahashi's solutions are classified to three types in accordance with the number of cells and play the role of the missing links in the sense that, by changing one of the parameters, metamorphoses take place from one types to another by connecting the Burgers' and Sullivan's vortices. Incorporation of boundaries is straightforward (Takahashi 2015a).

One may wonder how the simple vortices can be a model of typhoon if we recall that the real

typhoons are maintained by means of heat supply triggered by the conditional instability on air with moisture (Charney and Eliassen 1963 ; Ooyama 1966). Interestingly enough, the maintenance by heat has already been implicitly assumed in the simple vortices (Rott 1959 ; Takahashi 2015a, 2016). Furthermore, under appropriate boundary conditions, the temperature distribution within simple vortex has been shown to be quite similar to the ones observed in real typhoon (Takahashi 2015a, 2016). Exploiting simple vortices for understanding typhoon thus seems plausible. Of course, generation of heat from moisture and ensuing precipitation are essential ingredients of typhoon, as is supported partly by observations that typhoons frequently weaken after landing. However, elaborating their mechanism is another issue.

The linear perturbation on a simple vortex will be treated in more transparent way than the traditional numerical method (Takahashi 2013). In fact, the coordinate dependent eigenfrequencies satisfy a fourth-order algebraic equation, once the axisymmetric background velocity field was given. All of the four solutions do not diverge at infinity and can bear physical meanings, among which an unstable mode always exists.

Thus, one may address a question of whether the stability analysis of simple vortices can clarify the nature of unstable modes through mathematically tractable solutions of the eigenvalue problem in more general circumstances than the ones considered in Takahashi (2013). If the answer is affirmative, then it may help gain an insight into understanding the matured or evolving typhoon. External or internal disturbances like geographical irregularities or gas-liquid phase transition will serve as the seeds of perturbations (Charney and Eliassen 1963 ; Ooyama 1966), although we do not argue here the problems associated to these factors.

In this paper, the perturbative model employed by Takahashi (2013) is extended so as to incorporate gravity in a uniformly rotating frame that produces the Coriolis force. Gravity and frame rotation are ubiquitous conditions that are imposed on large scale swirling of fluid on heavenly bodies (Takahashi 2015b, 2015c, 2016 and references cited therein). Taking advantage of the Cheshire cat effect that the effect of viscosity is preserved after the zero limit of viscosity (Takahashi 2015a), the radial and the z-components of the velocity field are treated to be proportional to viscosity ν and are therefore infinitesimally small, while the azimuthal component is independent of ν.

This paper is organized as follows. In the next section, the EFE is derived for the rotating system under a uniform gravity. In sec. 3, the EFE is solved and the conditions for physical eigenfrequencies are sought analytically. In sec. 4, the EFE is numerically solved for some lower modes and for small Coriolis parameters. In sec. 5, large Coriolis parameters are taken into account in solving the

EFE with finite gravity.　In sec. 6, the relative amplitudes of stable and unstable modes are numerically found.　A summary is presented in sec. 7.　Derivation of the EFE is elaborated in the appendix.

2.　Linear perturbation and the EFE

The gravity is assumed to be uniform and acts along the z-direction in the cylindrical coordinate system (r, θ, z).　The perturbations around a steady and axisymmetric background flow ($v_r=v_z=0$, $v_\theta>0$) with a uniform density ρ under the presence of gravity g and the frame rotation obey in cylindrical coordinate the following equations

$$\left(\partial_t+\frac{v_\theta}{r}\partial_\theta\right)\delta v_r-\frac{2v_\theta\delta v_\theta}{r}=f\delta v_\theta-\frac{1}{\rho}\partial_r\delta p+\left(\frac{v_\theta^2}{r}+fv_\theta+\frac{f^2r}{2}\right)\frac{\delta\rho}{\rho}, \tag{2.1}$$

$$\left(\partial_t+\frac{v_\theta}{r}\partial_\theta\right)\delta v_\theta+\left(\partial_r v_\theta+\frac{v_\theta}{r}\right)\delta v_r=-f\delta v_r-\frac{1}{\rho r}\,\partial_\theta\delta p, \tag{2.2}$$

$$\left(\partial_t+\frac{v_\theta}{r}\partial_\theta\right)\delta v_z=-\frac{1}{\rho}\partial_z\delta p-g\frac{\delta\rho}{\rho}, \tag{2.3}$$

$$\left(\partial_t+\frac{v_\theta}{r}\partial_\theta\right)\delta\rho+\rho\left(\frac{1}{r}\delta v_r+\partial_r\delta v_r\right)+\frac{\rho}{r}\partial_\theta\delta v_\theta+\rho\partial_z\delta v_z=0. \tag{2.4}$$

The perturbations are denoted by the symbol δ.　f is the Coriolis parameter.　(2.4) is the continuity equation.　The meanings of the other symbols may be obvious.　In the above equations, the derivatives of the background velocity fields, the density and the pressure with respect to θ have been dropped.　Such axisymmetric velocity fields are constructed by the v-expansion method, which is reviewed in Appendix.

As usual, we assume that the components of the perturbations have a 'Fourier factor' and write

$$\delta v_r=R\exp[i(n\theta+kz-\omega t)], \tag{2.5a}$$

$$\delta v_\theta=\Theta\exp[i(n\theta+kz-\omega t)], \tag{2.5b}$$

$$\delta v_z=Z\exp[i(n\theta+kz-\omega t)], \tag{2.5c}$$

$$\delta p=\rho P\exp[i(n\theta+kz-\omega t)], \tag{2.5d}$$

$$\delta\rho=\rho D\exp[i(n\theta+kz-\omega t)], \tag{2.5e}$$

where n is an integer.　(The definitions of amplitudes are changed from those in Takahashi 2013.)

Now, we assume that the angular velocity ω and the amplitudes are r-dependent.　Substituting (2.5) to (2.1) ~ (2.4), we have

$$i(-\omega+n\Omega)R-2\Omega\Theta=f\Theta-(P'-i\omega' tP)+r\Omega^2\xi D, \tag{2.6}$$

$$i(-\omega+\Omega n)\Theta+(r\Omega'+2\Omega)R=-fR-\frac{in}{r}P, \tag{2.7}$$

$$\partial_t Z+i(-\omega+\Omega n)Z=-ikP-gD, \tag{2.8}$$

$$\partial_t D+i(-\omega+n\Omega)D=\left(\frac{1}{r}R+R'-i\omega' tR\right)+\frac{in}{r}\Theta+ikZ=0, \tag{2.9}$$

where $\Omega\equiv v_\theta/r$ and $\xi=1+f/\Omega+f^2/2\Omega^2$. The prime stands for a derivative by r. We assume that Ω continuously approaches zero for $r\to\infty$. In the above, D and Z are exceptionally assumed to be t-dependent in order to cancel the terms linear in t in (2.6) and (2.9). In order for such cancellations to occur, D and Z must be linear in t, too :

$$D=D^{(0)}+D^{(1)}t, \tag{2.10a}$$

$$Z=Z^{(0)}+Z^{(1)}t. \tag{2.10b}$$

Collecting the terms linear in t, we have

$$i\omega' P+r\Omega^2\xi D^{(1)}=0, \tag{2.11a}$$

$$\tilde{\omega}iZ^{(1)}=gD^{(1)}, \tag{2.11b}$$

$$D^{(1)}=-\frac{\omega'}{\tilde{\omega}}R+\frac{k}{\tilde{\omega}}Z^{(1)}, \tag{2.11c}$$

where $\tilde{\omega}\equiv\omega-n\Omega$. From these equations, P, $D^{(1)}$ and $Z^{(1)}$ are solved in terms of R :

$$iZ^{(1)}=-\frac{g\omega'}{\tilde{\omega}^2 ikg}R, \tag{2.12a}$$

$$D^{(1)}=-\frac{\omega'\tilde{\omega}}{\tilde{\omega}^2+ikg}R, \tag{2.12b}$$

$$iP=r\Omega^2\xi\frac{\tilde{\omega}}{\tilde{\omega}^2+ikg}R. \tag{2.12c}$$

Similarly, the t^0 terms yield

$$-i\tilde{\omega}R-(2\Omega+f)\Theta=-P'+r\Omega^2\xi D^{(0)}, \tag{2.13a}$$

$$\tilde{\omega}i\Theta-(r\Omega'+2\Omega+f)R=\frac{n}{r}iP, \tag{2.13b}$$

$$\tilde{\omega}Z^{(0)}=-iZ^{(1)}+kP-giD^{(0)}, \tag{2.13c}$$

$$D^{(1)}-i\tilde{\omega}D^{(0)}+\frac{1}{r}R+R'+\frac{n}{r}i\Theta+ikZ^{(0)}=0. \tag{2.13d}$$

For seven unknown amplitudes, we have two differential equations (2.13a) and (2.13d), or

$$P'=i\tilde{\omega}R+(2\Omega+f)\Theta+r\Omega^2\xi D^{(0)}, \tag{2.14a}$$

$$R' = -\frac{1}{r}R - D^{(1)} + i\tilde{\omega}D^{(0)} - \frac{n}{r}i\Theta - ikZ^{(0)}, \tag{2.14b}$$

with five constraints, i.e., (2.12) and

$$i\Theta = \left(\frac{r\Omega' + 2\Omega + f}{\tilde{\omega}} + \frac{n\Omega^2\xi}{\tilde{\omega}^2 + ikg}\right)R, \tag{2.15a}$$

$$Z^{(0)} = \frac{1}{\tilde{\omega}}\left[\frac{g\omega' - ikr\Omega^2\xi\tilde{\omega}}{\tilde{\omega}^2 + ikg}R - giD^{(0)}\right], \tag{2.15b}$$

obtained from (2.13b) and (2.13c), respectively. Note that $\tilde{\omega}$ and $\tilde{\omega}^2 + igk$ have been assumed to be non-zero. (It is easy to see that neither $\tilde{\omega} = 0$ nor $\tilde{\omega}^2 + igk = 0$ yields physically meaningful solutions.) The solutions exist for particular eigenfrequencies. We proceed the way similar to the one expounded in Takahashi (2013).

First, differentiate (2.12c) by r :

$$iP' = \frac{r\Omega^2\xi\tilde{\omega}}{\tilde{\omega}^2 + ikg}R' + \left(\frac{r\Omega^2\xi\tilde{\omega}}{\tilde{\omega}^2 + ikg}\right)'R. \tag{2.16}$$

Substitute (2.14b) to (2.16) to eliminate R'

$$iP' = r\left(\frac{\Omega^2\xi\tilde{\omega}}{\tilde{\omega}^2 + ikg}\right)'R + \frac{r\Omega^2\xi\tilde{\omega}}{\tilde{\omega}^2 + ikg}\left(-D^{(1)} + \tilde{\omega}iD^{(0)} - \frac{n}{r}i\Theta - ikZ^{(0)}\right). \tag{2.17}$$

P' is eliminated from (2.14a) and (2.17) to obtain

$$\left[\tilde{\omega} + r\left(\frac{\Omega^2\xi\tilde{\omega}}{\tilde{\omega}^2 + ikg}\right)'\right]R - \left(\frac{r\Omega^2\xi\tilde{\omega}}{\tilde{\omega}^2 + ikg} + 2\Omega + f\right)i\Theta - \frac{r\Omega^2\xi}{\tilde{\omega}^2 + ikg}\left(-kgD^{(0)} + \tilde{\omega}D^{(1)} + ik\tilde{\omega}Z^{(0)}\right) = 0. \tag{2.18}$$

Θ, $D^{(0)}$, $D^{(1)}$ and $Z^{(0)}$ in (2.18) are eliminated with helps of (2.12b), (2.15a) and (2.15b) to obtain the equation involving R only :

$$\left[\tilde{\omega} + r\left(\frac{\Omega^2\xi\tilde{\omega}}{\tilde{\omega}^2 + ikg}\right)'\right]R - \left(\frac{r\Omega^2\xi\tilde{\omega}}{\tilde{\omega}^2 + ikg} + 2\Omega + f\right)\left(\frac{n\Omega^2\xi}{\tilde{\omega}^2 + ikg} + \frac{r\Omega' + 2\Omega + f}{\tilde{\omega}}\right)R$$
$$- \frac{r\Omega^2\xi}{(\tilde{\omega}^2 + ikg)^2}(-\tilde{\omega}^2\omega' + ikg\tilde{\omega} + k^2r\Omega^2\xi\tilde{\omega})R = 0.$$

Then, recalling $\omega = \tilde{\omega} + n\Omega$ and requiring R to be nonzero lead to the following equation :

$$\tilde{\omega} - \frac{nr\Omega'\Omega^2\xi}{\tilde{\omega}^2 + ikg} + \frac{2nr\Omega'\Omega^2\xi\tilde{\omega}^2}{(\tilde{\omega}^2 + ikg)^2} + \frac{r(\Omega^2\xi)'\tilde{\omega}}{\tilde{\omega}^2 + igk}$$
$$- \left(\frac{n\Omega^2\xi\tilde{\omega}}{\tilde{\omega}^2 + igk} + 2\Omega + f\right)\left(\frac{n\Omega^2\xi}{\tilde{\omega}^2 + igk} + \frac{r\Omega' + 2\Omega + f}{\tilde{\omega}}\right)\frac{(kr\Omega^2\xi)^2\tilde{\omega}}{(\tilde{\omega}^2 + ikg)^2} = 0. \tag{2.19}$$

Note that ω' has also been entirely eliminated from (2.19). Multiplying $\tilde{\omega}(\tilde{\omega}+igk)^2$ to both sides of (2.19) and rearranging the terms, we have

$$\begin{aligned}\tilde{\omega}^6+(2igk-(2\Omega+f)(r\Omega'+2\Omega+f))\tilde{\omega}^4-2n\Omega^2\xi(2\Omega+f)\tilde{\omega}^3\\ -\left((n^2+k^2r^2)(\Omega^2\xi)^2+2igk(2\Omega+f)(r\Omega'+2\Omega+f)+g^2k^2\right)\tilde{\omega}^2\\ -2ingk\Omega^2\xi(r\Omega'+2\Omega+f)\tilde{\omega}+g^2k^2(2\Omega+f)(r\Omega'+2\Omega+f)=0.\end{aligned} \tag{2.20a}$$

This expression is simplified by noting that

$$\Omega=v_\theta/r=u_\theta/r-f/2\equiv\Omega_0-f/2$$

as

$$\begin{aligned}\tilde{\omega}^6+(2igk-2\Omega_0(r\Omega_0'+2\Omega_0))\tilde{\omega}^4-4n(\Omega_0^2+f^2/4)\Omega_0\tilde{\omega}^3\\ -((n^2+k^2r^2)(\Omega_0^2+f^2/4)^2+4igk\Omega_0(r\Omega_0'+2\Omega_0)+g^2k^2)\tilde{\omega}^2\\ -2ingk(\Omega_0^2+f^2/4)(r\Omega_0'+2\Omega_0)\tilde{\omega}+2g^2k^2\Omega_0(r\Omega_0'+2\Omega_0)=0.\end{aligned} \tag{2.20b}$$

This is the exact result within the linear theory of inviscid fluid. We have started with the equations involving ω'. However, ω' has finally disappeared, which renders the EFE (2.20) a pure algebraic equation. This is contrasted with that of McWilliams et al. (2003) where azimuthally averaged perturbations were considered and a differential equation for ω was derived. Fritts and Alexander (2003) studied the effects of gravity and Coriolis force within linear perturbation and found the fourth-order algebraic equation for the eigenfrequency. Their analysis relied on the WKB approximation (rapid oscillations of the phase and slow variations of the amplitudes) and thereby casts a doubt on the validity region.

The Coriolis parameter f appears in (2.20) with its quadratic powers. When f is far smaller than Ω, therefore, neglecting f in (2.20) will be a good approximation for finding $\tilde{\omega}$. In this case, the effect of the Coriolis force emerges in the background flow via. $v_\theta=u_\theta-fr/2$, where u_θ is the well-known vortex flow in a static frame of reference. See Appendix for details.

3. Finding physical eigenfrequencies

The EFE (2.20) is a sixth order algebraic equation and generally has six roots, whose precise analytical properties are hardly known. However, some limiting cases are rather tractable. Below, we shall take a look at them before performing numerical calculations.

3.1　$n=0$

In this case, (2.20) is rewritten as

$$(\tilde{\omega}^2+igk)^2(\tilde{\omega}^2-2\Omega_0(r\Omega_0'+2\Omega_0))=(kr(\Omega_0^2+f^2/4))^2\tilde{\omega}^2. \tag{3.1}$$

Let us remember that $\Omega_0\sim$ constant $+r^2$ near $r=0$ and $\sim r^{-2}$ at infinity. Then, if $f=0$, the r.h.s. may be neglected in the whole region of r because the r.h.s. behaves as r^2 near $r=0$ and r^{-6} at infinity. Thus, we have four approximate roots

$$\omega=\pm\sqrt{-igk},\pm\sqrt{2\Omega_0(r\Omega_0'+2\Omega_0)},(f=0). \tag{3.2}$$

The last two solutions rapidly vanish at infinity because $r\Omega_0'+2\Omega_0\to r^{-4}$ for $r\to\infty$.

Next consider the case $f\neq 0$ Near $r=0$, neglecting the r.h.s., we have

$$\tilde{\omega}=\pm\sqrt{-igk},\pm 2\Omega_0,(r\approx 0). \tag{3.3}$$

As a matter of course, the effect of the frame rotation has disappeared. At long distances, $2\Omega_0(r\Omega_0'+2\Omega_0)$ is again neglected but $f^2/4$ on the r.h.s. must be retained. Then, we have

$$\omega=0,\pm\sqrt{-igk\pm(f^2/4)kr},(r\to\infty). \tag{3.4}$$

3.2　$n\geq 1$

We consider the two limiting cases, i.e., $r=0$ and $r\to\infty$.

i)　$r=0$

$k^2r^2$and $r\Omega_0'$ vanish. The remaining equation is factorizable and reduces to

$$\tilde{\omega}(0)^3\pm 2\Omega_0(0)\tilde{\omega}(0)^2+\left(igk\pm n(\Omega_0(0)^2+f^2/4)\right)\tilde{\omega}(0)\pm 2igk\Omega_0(0)=0. \tag{3.5}$$

The exact roots will be found by Cardano's formula. For $|igk|\gg|n(\Omega_0(0)^2+f^2/4)|$, the roots are given by (3.3). Under the opposite condition, namely $|igk|\ll|n(\Omega_0(0)^2+f^2/4)|$, solutions are given by

$$\tilde{\omega}(0)=\begin{cases}\mp 2igk\Omega_0(0)/\left\{igk\pm n(\Omega_0(0)^2+f^2/4)\right\},\\ \mp\Omega_0(0)+\sqrt{-igk+(1\mp n)\Omega_0(0)^2-nf^2/4},\\ \mp\Omega_0(0)-\sqrt{-igk+(1\mp n)\Omega_0(0)^2-nf^2/4}.\end{cases} \tag{3.6}$$

The order of the double signs in (3.6) corresponds to the one in (3.5). Sufficiently large $\Omega_0(0)$or f give rise to, irrespective of k, an imaginary part in $\omega(0)$.

ii) $r \to \infty$

Noting that $\Omega_0, r\Omega_0' \to 0$, we may retain the highest order term and k^2r^2 term to have

$$\tilde{\omega}^6 + 2igk\tilde{\omega}^4 - g^2k^2\tilde{\omega}^2 = 0,\ f = 0. \tag{3.7a}$$

$$\tilde{\omega}^6 + (f/2)^4k^2r^2\tilde{\omega}^2 = 0,\ f \neq 0. \tag{3.7b}$$

The roots are

$$\omega(r \to \infty) = \begin{cases} n\Omega_0, \pm\sqrt{-igk}, & f = 0, \\ n\Omega_0, \pm(f/2)\sqrt{\pm kr} & f \neq 0. \end{cases} \tag{3.8}$$

The first one for each of two cases is the double roots. Note that (3.8) is independent of n and that, when $f \neq 0$, the effect of the gravity has disappeared.

Are the six roots all physically meaningful ? The answer to this question is found by constructing the amplitude equation and by scrutinizing it.

The amplitudes of the perturbations are determined by the equations presented in sec. 2. Let us consider R , the amplitude of δv_r. One can eliminate $D^{(1)}$, Q, $Z^{(0)}$ from (2.14b) with references to (2.12b), (2.15a) and (2.15b) together with the definition $\Omega = \Omega_0 - f/2$ to obtain

$$\frac{R'}{R} = \frac{1}{r} + \frac{\omega'\tilde{\omega}^2 - igk}{\tilde{\omega}\tilde{\omega}^2 + igk} - \frac{n}{r}\frac{r\Omega_0' + 2\Omega_0}{\tilde{\omega}} - \frac{\Omega_0^2 + f^2/4}{\tilde{\omega}^2 + igk}\left(\frac{n^2}{r} + k^2r\right) + i\left(\tilde{\omega} + \frac{igk}{\tilde{\omega}}\right)\frac{D^{(0)}}{R}. \tag{3.9}$$

Using ω determined by the method described above, the amplitude R is calculated from (3.9) once $D^{(0)}$ together with an appropriate boundary condition is posed.

Let us first consider the case $n = 0$. The first term on the r.h.s. of (3.9) gives rise in R to a term proportional to $1/r$. The divergence of R at $r = 0$ would cause a physical difficulty and should be deleted. The second and fourth terms are the ones employable for such a cancellation *if the first two solutions in (3.2) are adopted*. In fact, if the expression

$$\omega = \pm\left(\sqrt{-igk} + c_2r^2 + \cdots\right) \tag{3.10}$$

near $r = 0$ is employed, we have

$$\frac{\omega'\tilde{\omega}^2 - igk}{\tilde{\omega}\tilde{\omega}^2 + igk} \approx \frac{2c_2r}{\sqrt{-igk}}\frac{-2igk}{2\sqrt{-igk}\,c_2r^2} = \frac{2}{r},$$

$$\frac{\Omega_0(0)^2 + f^2/4}{\tilde{\omega}^2 + igk}k^2r \approx \frac{\Omega_0(0)^2 + f^2/4}{2\sqrt{-igk}\,c_2r^2}k^2r = -k^2\frac{\Omega_0(0)^2 + f^2/4}{2\sqrt{-igk}\,c_2r}.$$

Thus, collecting the most singular terms in (3.9), we have

$$\frac{R'}{R}=\frac{d_{-1}^{(0)}}{r}+\cdots, \tag{3.11a}$$

$$d_{-1}^{(0)}=1-\frac{|k|^2e^{2i\delta}}{2\sqrt{-igk}\,c_2}\left(\Omega_0(0)^2+\frac{f^2}{4}\right). \tag{3.11b}$$

The phases of $\sqrt{-igk}$ and c_2 will be correlated but, at present, we do not know how they are related. (c_2 is determined by using (2.20), which is a cumbersome task.) At least, one can say that the real part of the coefficient of $1/r$ can be greater than -1 by appropriately choosing $|k|$ and δ to delete the singularity in R. The above argument reveals that this is possible only when $\omega(0)=\pm\sqrt{-igk}$. This condition enables us to choose the physical branches from the six roots of (2.20) in case $n=0$. However, we have already seen that the solutions

$$\omega=\pm\sqrt{-igk},\ (n=0). \tag{3.12}$$

in (3.3), which satisfy the above condition, will be a good approximation in the whole region of r. Of course, in determining the amplitudes, higher order terms in (3.10) must be incorporated.

The above consideration also applies to the cases of $n\geq 1$: The correct branches are such that the solution of (3.9) does not diverge at $r=0$. Provided that neither $\tilde{\omega}(0)$ nor $\tilde{\omega}(0)^2+igk$ vanish, by collecting the r^{-1} terms and making use of (3.5), we find the coefficient of $1/r$ to be

$$\begin{aligned} d_{-1}^{(n)}&=-1-\frac{2n\Omega_0(0)}{\tilde{\omega}(0)}-\frac{n^2(\Omega_0(0)^2+f^2/4)}{\tilde{\omega}(0)^2+igk}\\ &=-1-\frac{2n\Omega_0(0)\tilde{\omega}(0)^2+n^2(\Omega_0(0)^2+f^2/4)\tilde{\omega}(0)+2ingk\Omega_0(0)}{\tilde{\omega}(0)(\tilde{\omega}(0)^2+igk)}\\ &=-1\pm n. \end{aligned} \tag{3.13}$$

The order of the signs is same as the one in (3.5). R is the perturbation amplitude for v_r that, owing to physical reason, must vanish at $r=0$, or $d_{-1}^{(n)}>0$. From (3.13), this is possible when $n\geq 2$ (≤ -2) for the upper (lower) signs in (3.5). Consequently, *the number of the spiral arms formed by internal perturbations is equal to or larger than two*.

If $\tilde{\omega}(0)^2+igk$ vanished, $1/r^2$ singularity would occur. However, numerical calculations show that this situation may be impossible.

The $D^{(0)}$ term is not determined within the N-S equations but gives the initial condition for the density perturbation. For instance, we may set $D^{(0)}=0$, i.e., the density perturbation does not initially exist.

4. Numerical calculations of eigenfrequencies

The eigenfrequencies for $n=0$ have been obtained as (3.12). Here we restrict ourselves to the cases of $n \geq 1$.

(2.19) generally has six complex roots specified by n and k. This equation is invariant for $n \to -n$, $\tilde{\omega} \to -\tilde{\omega}$ (or $\omega \to -\omega$), so that it is sufficient to restrict n to positive integers.

The effect of f will emerge when $f \geq \Omega_0$, i.e., at long radial distances. As was mentioned above, for practical purposes of studying phenomena on the earth, f may be safely neglected in determining ω. The case of large f will be argued later.

We have seen that $\tilde{\omega}(0) \neq 0$. More precisely, near the rotation axis, $\tilde{\omega}(r) \approx \tilde{\omega}(0) + \tilde{\omega}_2 r^2$ since Ω_0 is an even function of r.

The global properties of the solutions will be clarified by numerical calculations. For this purpose, we rewrite (2.20) in terms of new dimensionless functions and a variable $\tilde{\omega}(x) \equiv \tilde{\omega}/\sqrt{g|k|}$, $\hat{\Omega}(x) \equiv \Omega/\sqrt{g|k|} = v_\theta/\left(\sqrt{g|k|}\, r\right)$ and $x \equiv |k|r$ as

$$\hat{\omega}^6 + \left(2ie^{i\delta} - 2\hat{\Omega}_0\left(x\hat{\Omega}_0' + 2\hat{\Omega}_0\right)\right)\hat{\omega}^4 - 4n\hat{\Omega}_0^3\hat{\omega}^3 - \left((n^2 + e^{2i\delta}x^2)\hat{\Omega}_0^4 + 4ie^{i\delta}\left(x\hat{\Omega}\hat{\Omega}' + 2\hat{\Omega}^2\right) + e^{2i\delta}\right)\hat{\omega}^2$$
$$- 2ine^{i\delta}\hat{\Omega}_0^2\left(x\hat{\Omega}_0' + 2\hat{\Omega}_0\right)\hat{\omega} + 2e^{2i\delta}\hat{\Omega}_0\left(x\hat{\Omega}_0' + 2\hat{\Omega}_0\right) = 0, \tag{4.1}$$

where δ is the phase of k. The prime on $\hat{\Omega}_0$ stands for the derivative with respect to x.

Concerning the velocity field u_θ of the background flow, Takahashi (2014) showed that there exist three types of solutions, i.e., Type I, Type II and Type III, that are characterized by the number of cells (Sullivan 1959) and are mutually connected by continuous changes of parameters. In Fig. 1, three typical azimuthal velocities, labelled by I, II and III, are shown. $u_{\theta 1}$ is the Burgers solution (Burgers 1948)

$$\Omega_1 = \frac{\Gamma}{2\pi r^2}\left(1 - e^{-q^2 r^2}\right), \tag{4.2}$$

where Γ is the circulation at infinite distance. The angular velocities for other types asymptotically behave as (4.2) in case the circulation at infinity is the same.

We shall find the roots of (4.1) with the functional form (4.2) for Ω_0 parameterized so as for u_θ to have the peak velocity 40 m • s^{-1} at r = 30 km. Other parameter values are g = 9.8 m • s^{-2} and

$$k = -i/10 \text{ km}^{-1}, \ (\delta = -\pi/2) \tag{4.3}$$

The above values give $\sqrt{g|k|} = 0.0313\mathrm{s}^{-1}$. Following Fritts and Alexander (2003), we have chosen Imk to be negative so as for the perturbations to be amplified with altitude.

Among the six roots of (4.1), we select the ones that are the roots of the equation (3.5) with the upper signs. The results are shown in Fig. 2 for n = 1, 2 and 3.

There exist three branches – one is real and two are complex. The complex ones are mutually complex conjugate, so that the Reω for complex modes are degenerated and two curves for each n are drawn in the figure. The imaginary parts of the complex branches are constant and take the values of Im$\omega = \pm 0.990\ \mathrm{s}^{-1}$.

Other features are summarized below.

i) $n=1$: Reω of the complex modes and the neutral mode are almost symmetric about Re$\omega=0$. Namely, the complex modes propagate to the positive azimuthal direction (i.e., anti-clockwise), while the neutral mode to the opposite. The propagation speed decays with x, which means that the perturbations form trailing spirals. The decay or growth time of the complex modes are far shorter than the oscillation period.

ii) $n=2$: Reω of the neutral mode is zero and no propagations occur. Reω of the stable and unstable modes are positive and the perturbations propagate anticlockwise. At long distances they damp and vanish, so that the complex perturbations form trailing spirals.

iii) $n=3$: All three Reω exhibit similar properties to the ones for the complex $n=2$ modes.

In all cases mentioned above, the perturbations of the complex modes propagate faster than the neutral mode. In addition, we note that |Imω| is two order of magnitude larger than |Reω|. The growth velocity of the unstable perturbation is far faster than the oscillation rate.

The features of Reω markedly change when k has a real part. Examples for Rek = 0.02 km^{-1} ($\delta=-1.3734$) are shown in Fig. 3.

The degeneracies of Reω of complex modes are resolved. Reω is positive (negative) for stable (unstable) modes. This means that the perturbations of stable (unstable) mode azimuthally propagate anticlockwise (clockwise). Reω as functions of x become smoother with increase of δ. Although not shown here, this tendency gets more noticeable as the gravity and/or the vortex becomes stronger. In the cases shown in Fig. 3, Reω are almost constant. This means that the perturbations with nonvanishing Reω form a bar.

The constancy of ω is just the assumption commonly made in the WKB approximation. Based on

the observation presented above, we might conclude that the WKB approximation with this assumption is valid under the condition that the gravity is not too weak or the vortex is not too strong. The assumption of radially rapid oscillation of the phase is another ingredient of the WKB approximation. Whether this is really taking place is the matter remaining to be explored.

Each Reω rapidly approaches really a constant value beyond $x \approx 5$, which corresponds to $r \approx 50$ km. We note that, beyond this value of r, $u_{\theta \mathrm{I}}$ behaves as $1/r$, or $r\Omega_0' \sim \Omega_0 \approx 0$. Then, the asymptotic form (3.8) will apply. Therefore, altering the background flow is expected to bring about change of the features of ω we have seen so far.

In order to see the effect of changing the functional form of Ω by adopting different types of vortex, the solutions to (2.20) with $\Omega(r) = \Omega_{\mathrm{III}}(r) \equiv u_{\theta \mathrm{III}}(r)/r$ with $\max(u_{\theta \mathrm{III}}) = 40\ \mathrm{m \cdot s^{-1}}$ were sought. The results for $n = 1$, 2 and 3 are shown in Fig. 4. In all cases, the maxima of Reω are two order of magnitude greater than those shown in Fig. 2. This tendency remains true even when the original $u_{\theta \mathrm{III}}$ in Fig. 1 is adopted. Thus, we conclude that the unstable perturbation of Type III vortices grows far faster than those of Type I vortices.

We also notice that the graphical patterns of Reω of the stable modes mimic the background velocity fields.

5. Case of $f \neq 0$

The Coriolis parameter f is defined by $4\pi \sin\phi / p$, where p is the period of the rotation and ϕ the latitude. If f is nonzero, we have to deal with the whole of (2.20). By adopting the same normalization as the previous subsection, it is rewritten as

$$\begin{aligned} &\hat{\omega}^6 + \left(2ie^{i\delta} - 2\hat{\Omega}_0\left(x\hat{\Omega}_0' + 2\hat{\Omega}_0\right)\right)\hat{\omega}^4 - 4n\left(\hat{\Omega}_0^2 + \hat{f}^2/4\right)\hat{\Omega}_0\hat{\omega}^3 \\ &\quad - \left((n^2 + e^{2i\delta}x^2)\left(\hat{\Omega}_0^2 + \hat{f}^2/4\right)^2 + 4ie^{i\delta}\hat{\Omega}_0\left(x\hat{\Omega}_0' + 2\hat{\Omega}_0\right) + e^{2i\delta}\right)\hat{\omega}^2 \\ &\quad - 2ine^{i\delta}\left(\hat{\Omega}_0^2 + \hat{f}^2/4\right)\left(x\hat{\Omega}_0' + 2\hat{\Omega}_0\right)\hat{\omega} + 2e^{2i\delta}\hat{\Omega}_0\left(x\hat{\Omega}_0' + 2\hat{\Omega}_0\right) = 0, \end{aligned} \tag{5.1}$$

where $\hat{f} \equiv f/(g|k|)^{1/2}$. Obviously, the feature of the solutions is governed by the relative magnitudes of 1, $\hat{\Omega}$ and $\hat{f}$. The analysis presented in the previous subsection applies to the case $\hat{f} \ll 1, \hat{\Omega}$.

$\hat{f}$ is the ratio of the Coriolis parameter to the period of pendulum with the length equal to the thickness of the fluid. The typical values of $\hat{f}$ in the atmosphere of some heavenly bodies are given in Table 1.

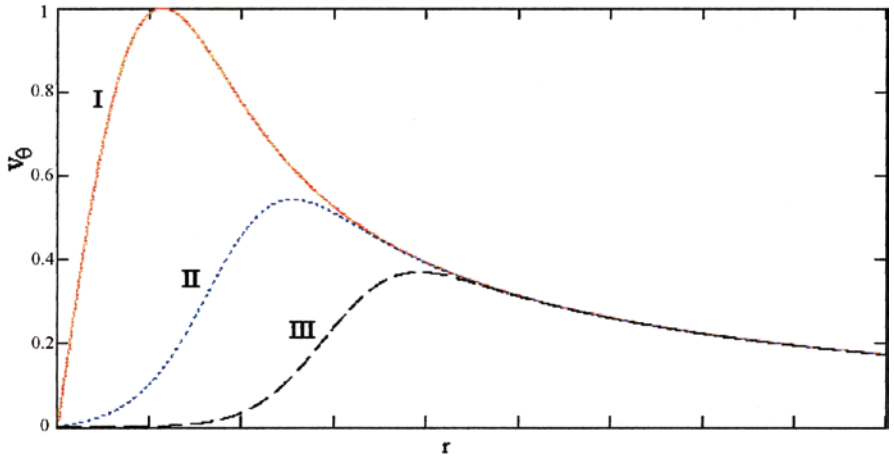

Fig. 1　Azimuthal flow velocity for three types of vortex solutions that have a common circulation at infinity. The curves labelled as I and II are the Burgers' (1948) and Sullivan's (1959) solutions and belong to Type I and II, respectively. The units of the distance and velocity are such that velocity labelled by I has a maximum 40 m • s^{-2} at $r = 30$ km. The curve labelled as III is an example of Type III solutions that were found by Takahashi (2014). These azimuthal velocities are used as u_θ in the text to calculate the eigenfrequencies.

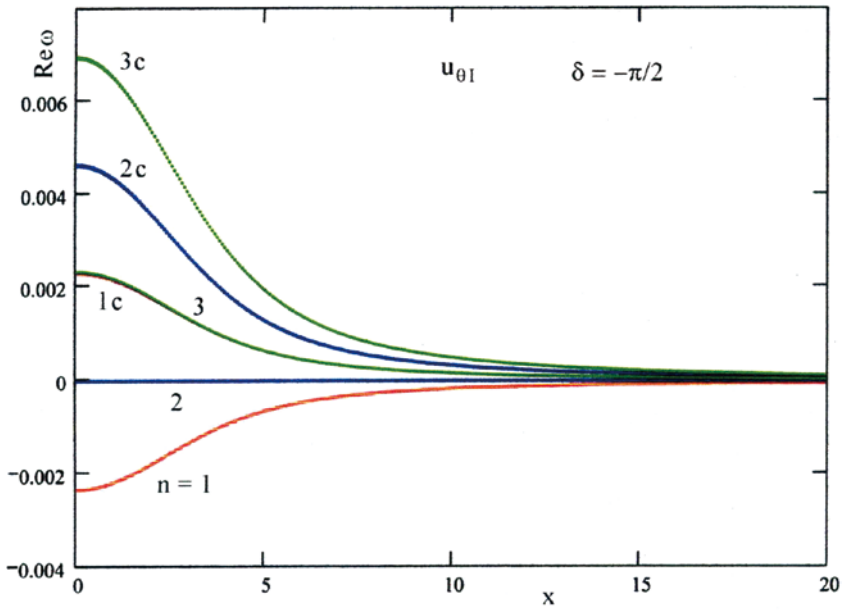

Fig. 2　Reω (in unit of s^{-1}) vs. x for $n = 1$(red), 2 (blue), 3 (green). Each curve is labelled by the azimuthal wave number together with 'c' which denotes complex modes. Complex modes consist of a stable (i.e., negative imaginary part) and an unstable (i.e., positive imaginary part) modes. For complex modes, Im$\omega = \pm 0.990$ s^{-1}. Parameters have been taken as $f = 0$ s^{-1}, $|k| = 0.1$ km^{-1}, $\delta = -\pi/2$ (i.e., Re$k = 0$). The velocity field I (Burgers vortex) in Fig. 1 has been employed.

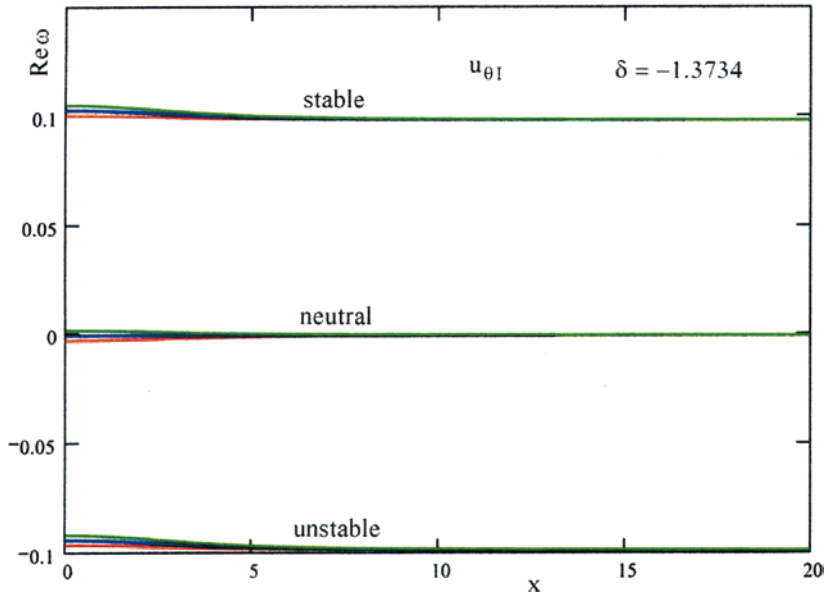

Fig. 3 Reω (in unit of s^{-1}) of modes $n=1$ (red), 2 (blue), 3 (green) for $k=0.02-0.1i$ km^{-1} ($\delta=-1.3734$), $f=0$ and are labelled by the azimuthal wave number. Complex and neutral branches are labelled by 'stable' or 'unstable' and 'neutral', respectively. Imω is 0.995 (-0.995) for Reω $<$ ($>$) 0. The velocity field I in Fig. 1 has been employed.

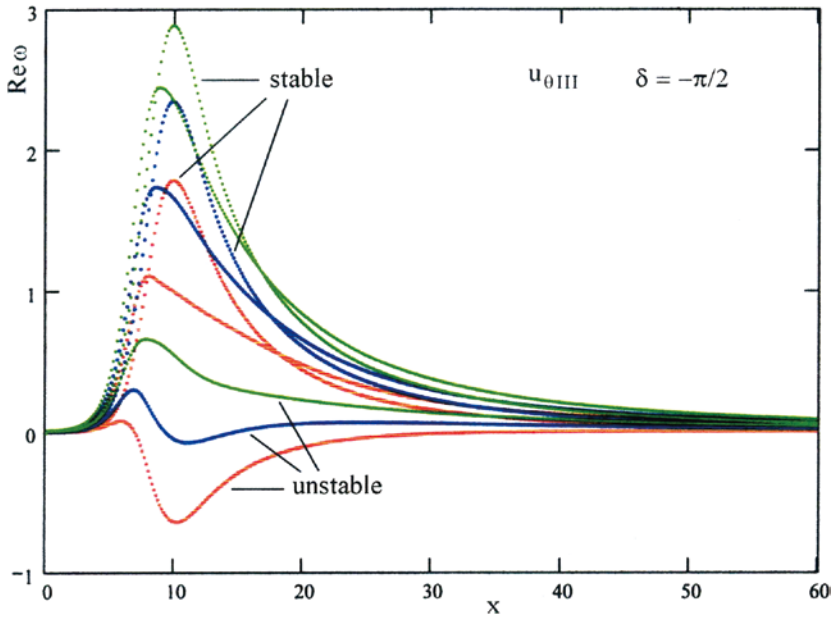

Fig. 4 Reω (in unit of s^{-1}) of mode $n=1$ (red curves), 2 (blue curves) and 3 (green curves) when the velocity field III in Fig. 1 with the same maximum velocity as $u_{\theta I}$ has been employed. For each n, three curves are drawn, among of which the one with the largest (smallest) maximum is of the stable (unstable) mode. The neutral mode lies in between. Parameters are $k=-0.1i$ km^{-1} ($\delta=-\pi/2$), $f=0$.

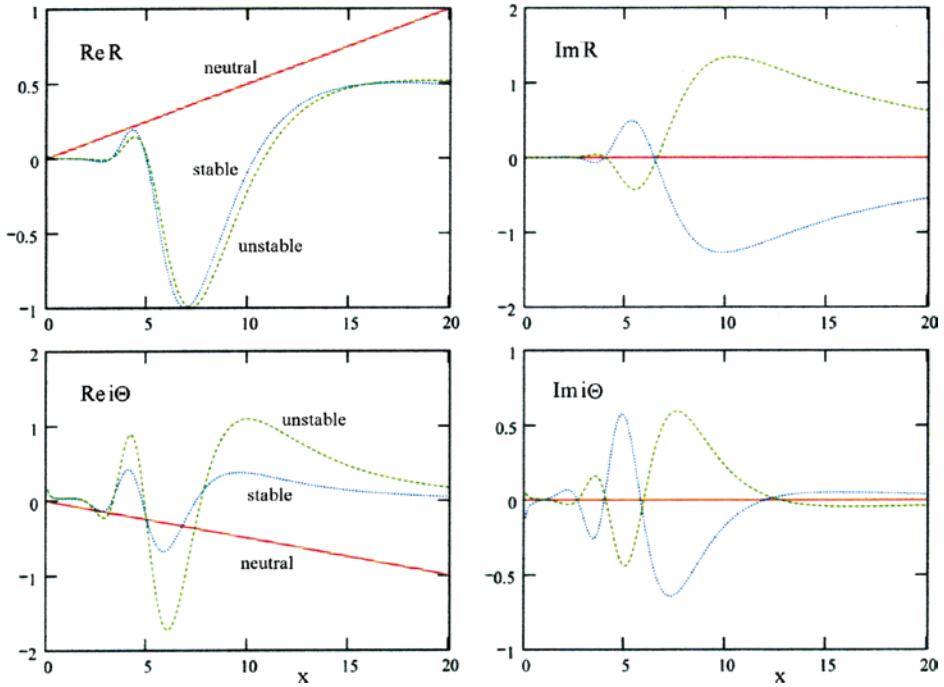

Fig. 5　Upper panels : ReR (left) and ImR (right) and lower panels : Re$i\Theta$ (left) and Im$i\Theta$ (right) for $n=2$, $D^{(0)}=0$ obtained by solving (3.9). Three curves are the solutions for ω's of neutral (solid curves), stable (dotted curves) and unstable (broken curves) modes are employed. $i\Theta$ for stable and unstable modes have been multiplied by 10^3. Normalizations to ReR are arbitrary, while, in other three panels, the ratios to max(Re | R |) are plotted. Parameters are given in the caption of Fig. 2.

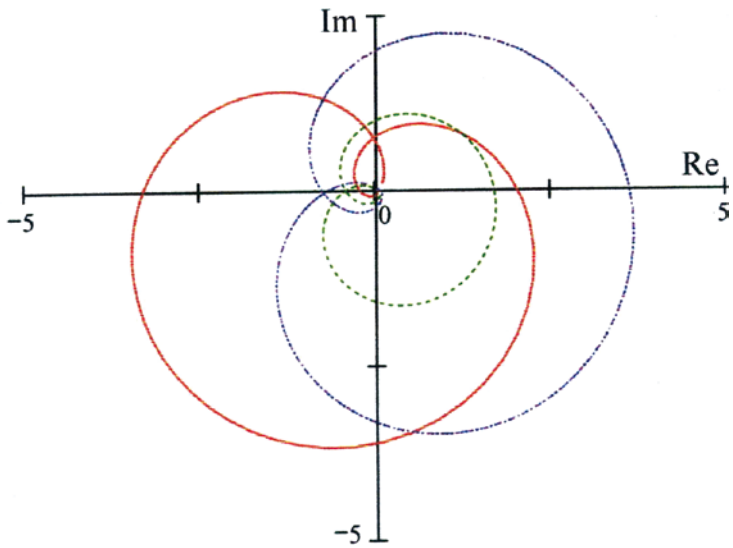

Fig.6.　Imaginary part vs. real part for unstable $Z^{(1)}$ (red solid curve), $Z^{(0)}$ (blue dotted curve), iP (green broken curve) and $D^{(1)}$ (purple dot-dashed curve). Normalization is max(| ReR |)=10. The curves for $Z^{(0)}$ and $D^{(1)}$ are completely overlapped on each other. The point on each curve moves clockwise from the origin to the origin along with the increase of x from 0 to infinity. iP has been multiplied by 100. Parameters are same as in Fig. 2.

Table 1 Radius R, rotation period p_r, $\tilde{f}$, g, thickness of atmosphere h, characteristic gravity frequency $f_g = (g|k|)^{1/2}$ and $\hat{f}$ of various heavenly bodies. Here, $\tilde{f}$ is defined by $2\pi/p_r$, $\hat{f}$ by $\tilde{f}/(g|k|)^{1/2}$ and k by $1/h$.

heavenly body	R (km)	p_r	$\tilde{f}$ (s^{-1})	g ($m \cdot s^{-2}$)	h (km)	f_g (s^{-1})	$\hat{f}$
Venus	6.1×10^3	243 d	3.0×10^{-7}	8.7	100	9.3×10^{-3}	3.2×10^{-5}
Earth	6.4×10^3	24 h	7.3×10^{-5}	9.8	10	3.1×10^{-2}	2.3×10^{-3}
Mars	3.4×10^3	24.5 h	7.1×10^{-5}	3.8	30	9.3×10^{-3}	6.3×10^{-3}
Sun	7×10^5	25.4 d	2.9×10^{-6}	270	1,000	1.2×10^{-2}	1.8×10^{-4}
neutron star	20	1 s	6.3	3.2×10^{11}	10^{-4}	1.8×10^{-6}	3.5×10^{-6}

$\hat{f} \ll 1$ in all cases in Table 1. Furthermore, in the examples exploited in the previous sections, $\hat{f} \ll |\hat{\Omega}(0)|$. Therefore, the Coriolis force is safely neglected for practical purposes. Exceptions are the long distance phenomena where the x^2 term in (5.1) gets significant or the case of very rapid rotation whose $\hat{f}$ is very large. The former case gives the second expression for ω in (3.8). In the followings, we examine the latter (maybe fictitious) case. (However, remember that, even for moderate f, $\hat{f}$ can be large for very small k.)

In order to see the large Coriolis effects, we here totally neglect the background velocity in (5.1). For simplicity, we restrict ourselves to the case $\delta = -\pi/2$. The roots of (5.1) are easily found as below.

1] $0 \le x < n$

i. If $n\hat{f}^2/4 > 1$, we divide the region into $0 \le x < x_c$ and $x_c \le x < n$, where $x_c \equiv \sqrt{n^2 - (2/\hat{f})^4}$. Then, except for $\hat{\omega} = 0$,

$$\hat{\omega} = \begin{cases} \pm\sqrt{(\hat{f}/2)^2\sqrt{n^2-x^2}-1}\,,\ \pm i\sqrt{(\hat{f}/2)^2\sqrt{n^2-x^2}+1}\,, & 0 \le x < x_c, \\ \pm i\sqrt{1\pm(\hat{f}/2)^2\sqrt{n^2-x^2}}\,, & x_c \le x < n. \end{cases}$$

At $x=0$, we have five possible values : $0, \pm\sqrt{(\hat{f}/2)^2 n - 1}, \pm i\sqrt{(\hat{f}/2)^2 n + 1}$. On the other hand, the physical solutions must satisfy (3.6). In the present case, it reads $\hat{\omega}(0) = 0,\ \pm i\sqrt{(\hat{f}/2)^2 n + 1}$. Therefore we adopt the last four roots in the above expressions, or

$$\hat{\omega} = \begin{cases} \pm i\sqrt{(\hat{f}/2)^2\sqrt{n^2-x^2}+1}\,, & 0 \le x < x_c, \\ \pm i\sqrt{1\pm(\hat{f}/2)^2\sqrt{n^2-x^2}}\,, & x_c \le x < n. \end{cases} \tag{5.2}$$

ii. If $n\hat{f}^2 - 4 \le 1$,

$$\hat{\omega} = \pm i\sqrt{1\pm(\hat{f}/2)^2\sqrt{n^2-x^2}}\,. \tag{5.3}$$

2]　$n \leq x$

$$\hat{\omega} = \pm\left(1+\left(\hat{f}/2\right)^4\left(x^2-n^2\right)\right)^{1/4} e^{\pm i\varphi/2},\ \varphi = \pi - \tan^{-1}\left(\left(\hat{f}/2\right)^2\sqrt{x^2-n^2}\right). \tag{5.4}$$

From (5.2) and (5.3), we see that only complex modes exist for $0 \leq x \leq n$. The following features for the present choice of δ is noticed :

(i) The neutral mode has ω which is given by $n\Omega_0$ at short distances and thus is a very slow mode.

(ii) At large distances, i.e., $x \gg n$, $\omega = \pm(1 \pm i)f\sqrt{x}\,/2\sqrt{2}$. Since $|\,\omega\,|$ monotonically increasing, perturbations form trailing or leading spirals.

(iii) The oscillation period of the unstable mode is same as the growth time at large distances.

6. Amplitudes of perturbation

The amplitudes of perturbation are determined by (3.9), (2.12) and (2.15), which, for convenience, are recapitulated below :

$$\frac{R'}{R} = -\frac{1}{r} + \frac{\omega'}{\tilde{\omega}}\frac{\tilde{\omega}^2 - igk}{\tilde{\omega}^2 + igk} - \frac{n}{r}\frac{r\Omega_0' + 2\Omega_0}{\tilde{\omega}} - \frac{\Omega_0^2 + f^2/4}{\tilde{\omega}^2 + igk}\left(\frac{n^2}{r} + k^2 r\right) + i\left(\tilde{\omega} + \frac{igk}{\tilde{\omega}}\right)\frac{D^{(0)}}{R}, \tag{3.9}$$

$$iZ^{(1)} = -\frac{g\omega'}{\tilde{\omega}^2 + ikg}R, \tag{2.12a}$$

$$D^{(1)} = -\frac{\omega'\tilde{\omega}}{\tilde{\omega}^2 + ikg}R, \tag{2.12b}$$

$$iP = r\left(\Omega_0^2 + \frac{f^2}{4}\right)\frac{\tilde{\omega}}{\tilde{\omega}^2 + ikg}R, \tag{2.12c}$$

$$i\Theta = \left(\frac{r\Omega_0' + 2\Omega_0}{\tilde{\omega}} + n\frac{\Omega_0^2 + f^2/4}{\tilde{\omega}^2 + ikg}\right)R, \tag{2.15a}$$

$$Z^{(0)} = \frac{g\omega'/\tilde{\omega} - ikr\left(\Omega_0^2 + f^2/4\right)}{\tilde{\omega}^2 + ikg}R - \frac{g}{\tilde{\omega}}iD^{(0)}. \tag{2.15b}$$

In our arguments, the initial density perturbation is assumed to be absent, i.e., $D^{(0)} = 0$. Apart from normalization, R is determined by the above set of equations once the background field, the azimuthal and vertical wavenumbers and the eigenfrequency are specified. We have seen that the azimuthal wavenumber is restricted as $n \geq 2$. (2.12a) implies that $Z^{(1)}$ is generally nonzero and the gravity causes the temporary linear growth of the vertical perturbation δv_z. This effect will emerge as the rapid growth of the vertical propagation rate of kinetic energy.

Now, we solve (3.9) for $n = 2$. Unfortunately, solving (3.9) is suffered from an obstacle that the

solution is very sensitive to the value of $\tilde{\omega}$ near $r=0$, while the roots of the EFE are accompanied with numerical errors that one cannot let small enough within the calculation method available to the present author. Nonetheless, we know that $R(0)$ must exactly vanish. Therefore, one is allowed to add a very small analytic function to the numerically determined ω so as for $|R(r)|$ near $r=0$ to become sufficiently small with keeping $\omega(r)$ be the solution of the EFE within our calculation precision in the whole region of r. The result is given in Fig. 5. The same background field and the parameters have been adopted as the ones in Fig. 2.

Three physical solutions corresponding to the stable, unstable and neutral modes exist. All three solutions smoothly approach zero as $r \to 0$. In intermediate region, the stable and unstable solutions slowly oscillate. Since $|k| = 0.1\ \mathrm{km}^{-1}$ in our valculations, their maxima are at about 150 km. This is a few times far outside of the eye wall of characteristic typhoon (The location of the eye wall has been set equal to 30 km from the symmetry axis).

Re R for the neutral mode increases with r approximately linearly. This is due to the smallness of ω as compared to Ω and $|igk|$.

Other amplitudes are calculated by using (2.12) and (2.15). We also give the result for $i\Theta$ in Fig. 5. By the same reasoning concerning R, $\Theta(0)$ must be zero. This is guaranteed by (2.15a), which, by virtue of (3.5), is written at $r=0$ as

$$i\Theta(0) = -R(0). \tag{6.1}$$

We here mention other strict conditions imposed on these amplituds. Since $\delta = -\pi/2$ in the present calculations, igk is real and all the coefficients of the equation (5.1) are real. Therefore, its two physical roots are mutually complex conjugate, which means that the corresponding two physical solutions to (3.9), (2.12) and (2.15), except for (2.15b), are also mutually complex conjugate. Consequently, in case the real parts are of the same signs, we have

$$\begin{aligned} &\mathrm{Re}\, R^{(\mathrm{s})} = \mathrm{Re}\, R^{(\mathrm{u})},\ \mathrm{Im}\, R^{(\mathrm{s})} = -\mathrm{Im}\, R^{(\mathrm{u})}, \\ &\mathrm{Re}\, i\Theta^{(\mathrm{s})} = \mathrm{Re}\, i\Theta^{(\mathrm{u})},\ \mathrm{Im}\, i\Theta^{(\mathrm{s})} = -\mathrm{Im}\, i\Theta^{(\mathrm{u})}, \end{aligned} \tag{6.2}$$

where the superscripts (s) and (u) denote stable and unstable mode, respectively. From Fig. 5, we see that the above conditions are less accurately satisfied for $i\Theta$ and the numerical precisions are quite limited. One should mainly heed functional tendencies.

One readily notice that u_θ is easily perturbed by the neutral mode. With reference to Fig. 2, we see that it will take a time of about $\ln(10^3)/0.002\ \mathrm{s} \approx 1$ hour around $x=5$ for the unstable mode to catch up

in magnitude with the neutral perturbation.

Concerning the other amplitudes, the curves of imaginary part vs. real part for unstable $Z^{(1)}$, $Z^{(0)}$, iP and $D^{(1)}$ are plotted in Fig. 6.

Note that the real and the imaginary parts of each amplitude are of the same order. However, concerning the amplitudes themselves, iP is 10^2 smaller than others (Remember that the amplitudes of the density and pressure perturbations have been defined by ρP and ρD). We have known that, when gravity is absent, the former are real and the latter are pure imaginary (Takahashi 2013). The gravity produces noticeable phase shifts for perturbation amplitudes.

When the radial velocity component locally varies, the mass conservation will necessarily give rise to the variation in the z-component, if fluid is incompressible. The result shown in Figs. 5 and 6 means that, for a compressible fluid, the response to local variation of v_r emerges as the change in v_θ, v_z and ρ.

7. Summary

The perturbations around the steady axisymmetric vortex with $v_r = v_z = 0$, $v_\theta \neq 0$ in a uniform gravity have eigenfrequencies ω that are determined by a sixth-order algebraic equation. Among its six roots, the three, each of which corresponds to neutral, stable or unstable mode, are physically acceptable. Perturbations with the azimuthal wavenumber being equal to or larger than 2 are possible. (This result may also be intriguing in connection with the galaxy dynamics.) v_θ, v_r, v_z and ρ acquire relatively large amplitudes as compared to P. The prominent effects of gravity emerge when the modulation in vertical direction exist. At first glance, the applicability of the WKB method may seem to be attained with the elapse of time, since the phase involves the term Reωt. However, it is dubious because the amplitudes of perturbations for the vertical velocity and the density also linearly increase with time.

Appendix Axisymmetric vortices in a rotating frame

1. Background field

The rotation of the reference frame is incorporated by introducing the Coriolis parameter f to the N-S equations, which are expressed as

$$\partial_t v_r + v_r \partial_r v_r + \frac{v_\theta}{r}\partial_\theta v_r + v_z \partial_z v_r - \frac{v_\theta^2}{r} = \nu\left(\nabla^2 v_r - \frac{v_r}{r^2} - \frac{2}{r^2}\partial_\theta v_\theta\right) - \frac{1}{\rho}\partial_r p + f v_\theta + F_r \tag{A1}$$

$$\partial_t v_\theta + \frac{v_r}{r}\partial_r (r v_\theta) + \frac{v_\theta}{r}\partial_\theta v_\theta + v_z \partial_z v_\theta = \nu\left(\nabla^2 v_\theta - \frac{v_\theta}{r^2} + \frac{2}{r^2}\partial_\theta v_r\right) - \frac{1}{\rho r}\partial_\theta p - f v_r + F_\theta \tag{A2}$$

$$\partial_t v_z + v_z \partial_r v_z + \frac{v_\theta}{r}\partial_\theta v_z + v_z \partial_z v_z = \nu \nabla^2 v_z - \frac{1}{\rho}\partial_z p + F_z. \tag{A3}$$

Solutions are sought with the condition of mass conservation

$$\partial_t \rho + \frac{1}{r}\partial_r (r \rho v_r) + \frac{1}{r}\partial_\theta (\rho v_\theta) + \partial_z (\rho v_z) = 0. \tag{A4}$$

Let us introduce a new variable u_θ by

$$v_\theta = u_\theta - fr/2. \tag{A5}$$

We further assume that all the quantities in (A1)~(A4) are stationary and axisymmetric. Then, (A1)~(A4) are reduced to

$$v_r \partial_r v_r + v_z \partial_z v_r - \frac{u_\theta^2}{r} - \frac{f^2 r}{4} = \nu\left(\nabla^2 v_r - \frac{v_r}{r^2}\right) = \frac{1}{\rho}\partial_r p + F_r, \tag{A6}$$

$$\frac{v_r}{r}\partial_r (r u_\theta) + v_z \partial_z u_\theta = \nu\left(\nabla^2 u_\theta - \frac{u_\theta}{r^2}\right), \tag{A7}$$

$$v_r \partial_r v_z + v_z \partial_z v_z = \nu \nabla^2 v_z - \frac{1}{\rho}\partial_z p + F_z, \tag{A8}$$

$$\frac{1}{r}\partial_r (r \rho v_r) + \partial_z (\rho v_z) = 0. \tag{A9}$$

The ν-expansion method assumes the forms $v_r = \nu v_{r1}$, $v_z = \nu v_{z1}$, $u_\theta = u_{\theta 0}$ for the velocity field, where v_{r1}, v_{z1}, $u_{\theta 0}$ are all independent of ν (Takahashi 2014). Substituting the above forms to (A6)~(A9) yields a set of equations for the quantities v_{r1}, v_{z1}, $u_{\theta 0}$. For examples, if $F_r = 0$, ν^0 terms yield

$$\frac{u_{\theta 0}^2}{r} + \frac{f^2 r}{4} = \frac{v_\theta^2}{r} + f v_\theta + \frac{f^2 r}{2} = \frac{1}{\rho}\partial_r p_0, \tag{A10}$$

$$0 = -\frac{1}{\rho}\partial_z p_0 + F_z. \tag{A11}$$

Here, $u_{\theta 0}$ is a function of r only. If $f^2 r/2$ on the middle part of (A10) is absorbed to the definition of p_0, then (A10) and (A11) are nothing but the balance equations employed in meteorological studies (e.g., Charney and Eliassen 1963). The full set of equations for the velocity field is equivalent to the one without the Coriolis term and gives various vortex solutions for (v_r, u_θ, v_z) (Takahashi 2014). The vortices are classified into Types I, II and III, in which Burgers' and Sullivan's ones are involved. In the inviscid limit, the velocity field reduces to (0, u_θ, 0).

2. Derivation of the EFE

Perturbations around $(0, v_\theta = u_\theta - fr/2, 0)$ obey, in inviscid limit, the equations

$$\left(\partial_t + \frac{v_\theta}{r}\partial_\theta\right)\delta v_r - \frac{2v_\theta \delta v_\theta}{r} = f\delta v_\theta - \frac{1}{\rho}\partial_r \delta p + \frac{\delta\rho}{\rho^2}\partial_r p, \tag{A1)'}$$

$$\left(\partial_t + \frac{v_\theta}{r}\partial_\theta\right)\delta v_\theta + \frac{\delta v_r}{r}\partial_r(rv_\theta) = -\frac{1}{\rho r}\partial_\theta \delta p - f\delta v_r, \tag{A2)'}$$

$$\left(\partial_t + \frac{v_\theta}{r}\partial_\theta\right)\delta v_z = -\frac{1}{\rho}\partial_z \delta p + \frac{\delta\rho}{\rho^2}\partial_z p, \tag{A3)'}$$

$$\left(\partial_t + \frac{v_\theta}{r}\partial_\theta\right)\delta\rho + \frac{1}{r}\partial_r(r\rho\delta v_r) + \frac{1}{r}\partial_\theta(\rho\delta v_\theta) + \partial_z(\rho\delta v_z) = 0. \tag{A4)'}$$

Together with (A10) and (A11) with $F_z = -g$ we have (2.1) ~ (2.4). Derivations of (2.19) and (2.20) are straightforward.

References

Burgers JM, 1948　A mathematical model illustrating the theory of turbulence. *Adv. Appl. Mech*. **1**, 171.

Charney JG and Eliassen A, 1963　On the growth of the hurricane depression. *J. Atmos. Sci.* **21**, 68.

Eady T, 1949　Long waves and cyclone waves. *Tellus* **1**, 33.

Fritts DC and Alexander MJ, 2003　Gravity wave dynamics and effects in the middle atmosphere, *Rev. Geophys*., **41**, 1003.

Holland GJ, 1980　An analytic model of the wind and pressure profiles in hurricanes. *Mon. Wea. Rev.* **106**, 1212.

McWilliams JC, Graves LP and Montgomery MT, 2003　A formal theory for vortex Rossby waves and vortex evolution. *Geophys. Astrophys. Fluid Dyn*. **97**, 275.

Nolan DS and Montgomery MT, 2002　Nonhydrostatic, three-dimensional perturbations to balanced, hurricane-like vortices. part I : linearized formulation, stability, and evolution. *J. Atmos. Sci.* **59**, 2989.

Ooyama K, 1966　Numerical simulation of the life cycle of tropical cyclones. *J. Atmos. Sci*. **26**, 3.

Rott N, 1959　On the viscous core of a line vortex II. *Z. angew. Math. Phys*. **X**, 73.

Sullivan RD, 1959　A two-cell vortex solution of the Navier-Stokes equations. *J. Aerosp. Sci*. **26**, 767.

Takahashi K, 2013　Multiple peaks of the velocity field as the linear perturbations on the non-Eulerian inviscid vortex. *Fac. Lib. Arts Rev.* (*Tohoku Gakuin Univ.*) **166**, 1 ; http://www.tohoku-gakuin.ac.jp/research/journal/bk2013/pdf/no10_02.pdf, date last accessed August 1, 2016).

Takahashi K, 2014　Classification of the steady axisymmetric vortices. *Fac. Lib. Arts Rev.* (*Tohoku Gakuin Univ.*) **168**, 51 ; http://www.tohoku-gakuin.ac.jp/research/journal/bk2014/pdf/no06_03.pdf

Takahashi K, 2015a　Simple vortices and typhoon. *Fac. Lib. Arts Rev.* (*Tohoku Gakuin Univ.*) **171**, 105 (in Japanese), http://www.tohoku-gakuin.ac.jp/research/journal/bk2015/pdf/no06_06.pdf, date last accessed August 1, 2016.

Takahashi K, 2015b　Application of the viscosity-expansion method to a rotating thin fluid disk bound by central gravity *PTEP* 073J01.

Takahashi K, 2015c　The effect of self-gravity in linearly perturbed Euler equations for a rotating thin fluid disk.　*Fac. Lib. Arts Rev.* (*Tohoku Gakuin Univ.*) **173**, 123, http://www.tohoku-gakuin.ac.jp/research/journal/bk2016/pdf/no02_05.pdf, date last accessed August 1, 2016.

Takahashi K, 2016　Erratum.　*Fac. Lib. Atys Rev*. (*Tohoku Gakuin Univ.*) **173**, 144 (in Japanese), http://www.tohoku-gakuin.ac.jp/research/journal/bk2016/pdf/no02_05.pdf, date last accessed August 1, 2016.

Walko R and Gall R, 1984　A two-dimensional linear stability analysis of the multiple vortex phenomenon.　*J. Atmos Sci.* **41**, 3456.

Willoughby HE and Rahn ME, 2004　Parametric representation of the primary hurricane vortex.　Part I : Observations and evaluation of the Holland (1980) model.　*Mon. Wea. Rev*. **132**, 3033.

Willoughby HE, Darling RWR and Rahn ME, 2005　Parametric representation of the primary hurricane vortex.　Part II : A new family of sectionally continuous profiles.　*Mon. Wea. Rev.* **134**, 1102.